Development 139, 1133-1140 (2012) doi:10.1242/dev.073478

An essential role for a mammalian SWI/SNF chromatin-remodeling complex during male meiosis

Yuna Kim, Andrew M. Fedoriw and Terry Magnuson*

SUMMARY

Germ cell development and gametogenesis require genome-wide transitions in epigenetic modifications and chromatin structure. These changes include covalent modifications to the DNA and histones as well as remodeling activities. Here, we explore the role of the mammalian SWI/SNF chromatin-remodeling complex during spermatogenesis using a conditional allele of the ATPase subunit, brahma-related gene 1 (*Brg1*, or *Smarca4*). Not only do BRG1 levels peak during the early stages of meiosis, genetic ablation of *Brg1* in murine embryonic gonocytes results in arrest during prophase of meiosis I. Coincident with the timing of meiotic arrest, mutant spermatocytes accumulate unrepaired DNA and fail to complete synapsis. Furthermore, mutant spermatocytes show global alterations to histone modifications and chromatin structure indicative of a more heterochromatic genome. Together, these data demonstrate a requirement for BRG1 activity in spermatogenesis, and suggest a role for the mammalian SWI/SNF complex in programmed recombination and repair events that take place during meiosis.

KEY WORDS: Chromatin remodeling, SWI/SNF, Mouse spermatogenesis, Meiosis, Mouse

INTRODUCTION

Mammalian gametogenesis requires numerous epigenetic changes to accompany the transition from somatic, diploid precursors to mature, haploid gametes (reviewed by Sasaki and Matsui, 2008). Embryonic epigenetic states are first erased and reprogrammed during the development of primordial germ cells (PGCs). Later, as germ cells differentiate and proceed through meiosis, their genomes undergo large-scale changes to histone and DNA modifications as well as chromatin structure. This transition is important for the progression through meiosis, which itself requires the action of macromolecular complexes to manage the series of events entailing meiotic recombination between homologous chromosomes. It is therefore not surprising that faithful execution of the meiotic program requires the action of a large number of epigenetic pathways. Recent work has identified DNA methyltransferases, histone-modifying enzymes, and RNA-binding proteins, which when inactivated by mutations, result in failure of spermatogenesis (Kota and Feil, 2010).

In both male and female germ cells, homologous recombination occurs during the first meiotic prophase. During this time DNA double-stranded breaks (DSBs) are induced, and repair at the DSBs generates DNA recombination between homologous chromosomes. Many of the factors required for repair of stress-induced DNA damage in somatic cells function during meiosis. In addition to their well-characterized roles in transcriptional regulation, chromatin-remodeling complexes have roles in DNA repair (Bao and Shen, 2007; Clapier and Cairns, 2009). Among them, members of the SWI/SNF ATP-dependent chromatin remodelers appear to have a conserved function in the DSB repair process in yeast (Chai et al., 2005) and human somatic cells (Park et al., 2006; Zhao et al., 2009). Upon induction of DNA damage by ionizing radiation, the SWI/SNF catalytic subunit BRG1 (SMARCA4 – Mouse Genome Informatics) is required for the phosphorylation of the histone variant γH2AX (H2AFX – Mouse Genome Informatics), which in turn promotes the recruitment of downstream repair proteins. These observations suggest a role for mammalian SWI/SNF remodeling complexes in the repair of stress-induced DNA damage; however, whether they also play a role in programmed DNA repair events, such as those during meiosis, is not yet known.

In this report, we show that a germline-specific ablation of *Brg1* results in a critical defect in spermatogenesis in the mouse. We demonstrate that BRG1 protein levels normally peak during the early phases of meiosis I. Consistent with this pattern, germ cells lacking BRG1 fail to complete prophase I. Although γH2AX appears normally induced in mutant spermatocytes, it persists into later stages of prophase I along with aberrant foci of repair proteins. BRG1-depleted spermatocytes showed significant deviation in the expected global patterns of epigenetic modifications, including those that are associated with DNA damage and heterochromatin. Together, these results demonstrate an essential role for BRG1 in spermatogenesis, and suggest a function for BRG1-containing complexes in homologous recombination during meiosis.

MATERIALS AND METHODS

Brg1 conditional deletion and genotyping

Mice carrying a floxed allele of *Brg1* (Sumi-Ichinose et al., 1997) and *Mvh-Cre* (Gallardo et al., 2007) were maintained on a mixed background. Mutant and normal littermates were obtained from crosses between female homozygous *Brg1flox* mice with male *Mvh-Cre/+; Brg1*$^{\Delta/+}$ mice. PCR genotyping primers for wild-type and floxed alleles of *Brg1* included: forward 5′-GCCTTGTCTCAAACTGATAAG and reverse 5′-GTCATACTTATGTCATAGCC; for the excised allele of *Brg1*, forward 5′-GATCAGCTCATGCCCTAAGG and the same reverse sequence; for *Cre*, forward 5′-CACGTGCAGCCGTTTAAGCCGCGT and reverse 5′-TTCCCATTCTAAACAACACCCTGAA. All animal work was carried out in accordance with IACUC protocols at UNC.

Department of Genetics, Carolina Center for Genome Sciences, Lineberger Comprehensive Cancer Center, University of North Carolina at Chapel Hill, NC 27599-7264, USA.

*Author for correspondence (trm4@med.unc.edu)

Accepted 9 January 2012

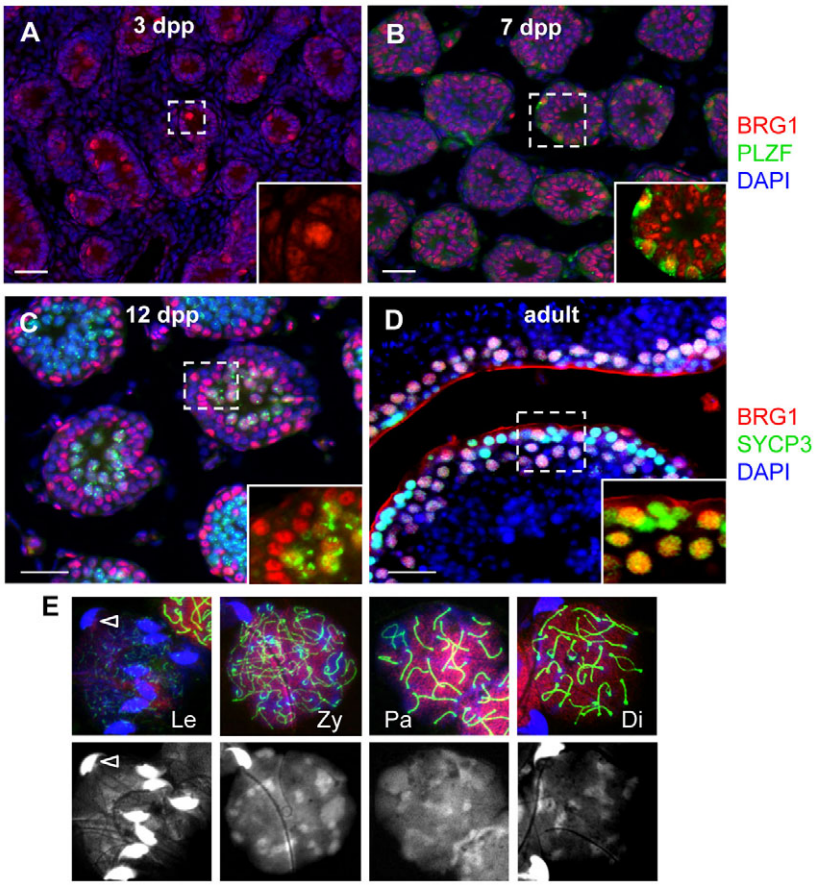

Fig. 1. BRG1 expression during spermatogenesis. (**A-D**) BRG1 (red) expression in neonatal testes at specified ages (A–C) and adult testis at 8 weeks (D). Insets show magnified views of the marked areas depicting BRG1 detection in prospermatogonia [round, large nuclei (A), PLZF-positive (green) spermatogonia (B), and SYCP3-positive (green) spermatocytes (C,D)]. (**E**) Double immunostaining of BRG1 (red) and SYCP3 (green) in nuclei spreads prepared from 8-week-old testis. Spermatocytes were staged based on the appearance of the synaptonemal complex in nuclear spreads (marked by SYCP3, green). Nuclear staining is enhanced by DAPI-only images (bottom panels). Bright and hooked nuclei (arrowhead) are sperm. In all images, nuclei were counterstained with DAPI (blue) unless otherwise specified. Scale bars: 50 μm. Di, diplonema; Le, leptonema; Pa, pachynema; Zy, zygonema.

Histological analysis

After dissection, testes were fixed in Bouin's fixative overnight at 4°C, dehydrated in an ethanol series, and embedded in paraffin wax. Sections were made at 3 μm thickness using a microtome. Following standard protocols, sections were deparaffinized, rehydrated, and then stained with Hematoxylin and Eosin for histology.

Immunofluorescence staining and antibodies

Preparation of testis cryosections and nuclear surface spreads of meiocytes were performed as described previously (Peters et al., 1997; Kim et al., 2007) with the following modifications. For the preparation of cryosections, tissues were washed in PBS at pH 7.4, permeabilized in PBST (PBS with 0.1% Triton X-100), and fixed in 4% paraformaldehyde in PBST overnight at 4°C. Fixed tissues were saturated through a sucrose series and embedded in optimal cutting temperature (OCT; Sakura Rinetek, Torrence, CA, USA). Frozen tissue sections were cut at 8 μm thickness. Slides were dried for 2 hours on a 37°C warming plate or overnight at room temperature (RT). An antigen retrieval step was required for several antibodies: slides were washed in PBT (PBS with 0.1% Tween 20), boiled in 10 mM citric acid (pH 6.0) for 10–30 minutes, and cooled slowly at RT for 1 hour.

For the preparation of nuclear spreads, seminiferous tubules were dissected and incubated for 20 minutes in a hypotonic extraction buffer (30 mM Tris pH 8.2; 50 mM sucrose; 17 mM citrate; 5 mM EDTA, 0.5 mM DTT; 0.1 mM PMSF). The tubule fragments were added to 100 mM sucrose solution to release hypotonized nuclei by pipetting repeatedly or mincing with a blade. A drop of nuclear suspension was spread onto slides coated with 1% paraformaldehyde. Slides were dried completely, washed in 0.4% Photo-Flo solution (Kodak), and dried again for storage. We categorized substages of prophase I by localization of the synaptonemal complex proteins SYCP3 and SYCP1, together with the kinetics of histone variant γH2AX distribution (Mahadevaiah et al., 2001).

For immunofluorescence staining, slides were blocked in 5% serum from the same species used for the secondary antibody for 1 hour at RT, incubated in primary antibodies at an optimized titer overnight at 4°C and subsequently in Alexa fluorophore conjugated secondary antibodies (Molecular Probes) for 1 hour at RT. The M.O.M. Immunodetection Kit (BMK-2202, Vector) was used as directed to eliminate background staining from endogenous mouse immunoglobulin. Nuclei were counterstained with 4,6-diamidino-2-phenylindole (DAPI, Sigma). For imaging, slides were mounted using an anti-quenching medium, ProlongGold (Invitrogen, P36930). Fluorescence microscopy was conducted using Leica DMLB or Zeiss Imager-M2 microscopes. Antibodies used in this study are: rabbit anti-BRG1 (1:100, Santa Cruz, sc-10768), monoclonal mouse anti-BRG1 (1:1000, Santa Cruz, sc-17796), rabbit anti-BRM (1:250, Abcam ab15597), rabbit anti-beta-galactosidase (1:500, Cappel #55976), rabbit anti-CRE (1:200, Covance, MMS-106R), mouse anti-γH2AX (1:800, Millipore #05-636), rabbit anti-phospho-HH3 (1:500, Cell Signaling #9701), mouse anti-histone H3 dimethylated lysine 9 (1:500, H3K9me2, Abcam ab1220), rabbit anti-histone H3 acetylated lysine 9 (1:500, H3K9Ac, Millipore #06-942), rabbit anti-histone H4 pan-acetylated (1:200, Millipore #06-866), rat anti-HP1β (1:500, Abcam ab10811), rabbit anti-HP1γ (1:500, Abcam ab66617), mouse anti-MLH1 (1:500 BD BioScience #51-1327GR), rabbit anti-MVH (1:5000, Abcam #13840), mouse anti-PLZF (1:100, Calbiochem #OP128), rabbit anti-RAD51 (1:250, Calbiochem PC130T; 1:100, Santa Cruz sc-8349), rabbit anti-RPA (1:100, Bethy Lab IHC-00409), rabbit anti-SCP1 (1:1000, Abcam ab15090), rabbit anti-SCP3 (1:500, Abcam ab15093), mouse anti-TRA98 (1:500, Cosmo Bio 73-003-EX). Secondary antibodies used were goat or donkey IgG conjugated with one of Alexa Fluor 488, 568 and 594 (Invitrogen). When applicable, we used secondary antibody matched for the isotypes.

Cell proliferation and apoptosis assay

Proliferating cells were detected by immunostaining with a mitotic marker. Histone H3 phosphorylated at serine 10 (pHH3) specifically labels cells in metaphase. For cell apoptosis analysis, fluorescent TUNEL assay was conducted by using the *In Situ* Cell Death Detection Kit (Roche, #11 684 795 001).

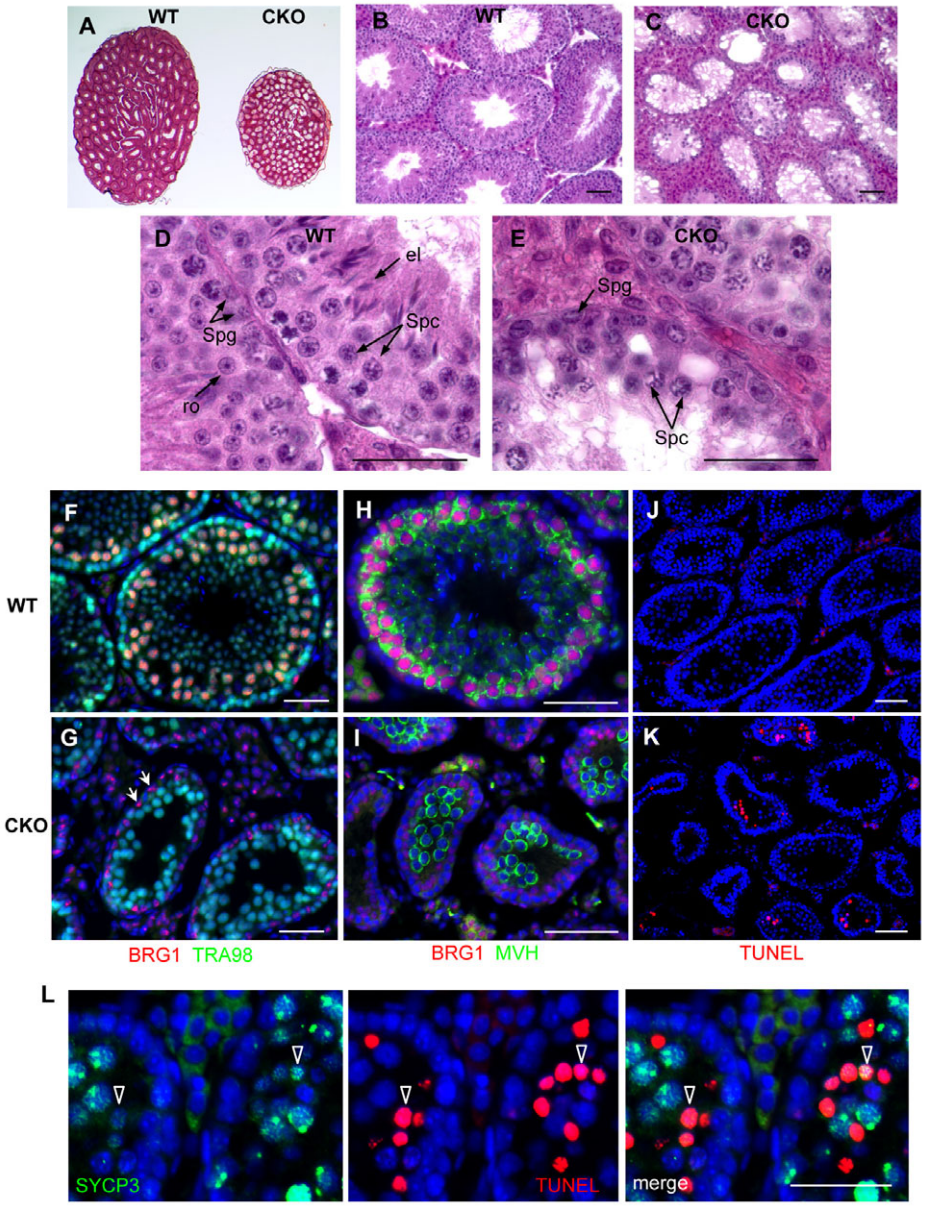

Fig. 2. Loss of spermatocytes and increased apoptosis in *Brg1*^{CKO} testes. (**A-E**) Hematoxylin and Eosin staining of wild-type (WT) and mutant (CKO) testes from 10-week-old mice. (**F**,**G**) Double immunostaining of BRG1 (red) and TRA98, a pan-germ cell marker (green), in 4-week-old wild-type (F) and *Brg1*^{CKO} (G) testes (Sertoli cells marked by arrows). (**H**,**I**) *Mouse vasa homolog* (MVH, green) activation in differentiating germ cells. (**J**,**K**) Fluorescence TUNEL assay of wild-type (J) and mutant (K) testes at 3 weeks. (**L**) Co-staining of TUNEL (red) with SYCP3 (green) in apoptotic *Brg1*^{CKO} spermatocytes. Scale bars: 50 μm. el, elongated spermatid; ro, round spermatid; Spc, spermatocyte; Spg, spermatogonia.

Statistical analyses

Chi-squared analysis was carried out to test differences in meiotic stage distribution in mutant and wild-type spermatocytes. A two-sided Fisher's exact test was used to determine significance of SYCP3, RAD51, RPA (RPA1 – Mouse Genome Informatics), MLH1 distribution patterns. At least two mice per genotype were used for each experiment.

RESULTS

BRG1 expression in male germ cells

To determine whether BRG1 plays a role in gametogenesis, we analyzed BRG1 expression during spermatogenesis by immunofluorescence staining. BRG1 was detected as early as 3 days post partum (dpp), when the prospermatogonia, the quiescent precursors to the spermatogonial stem cells, re-enter the cell cycle (Fig. 1A). BRG1 expression continued at 7 dpp (Fig. 1B) as prospermatogonia differentiate into spermatogonia marked by the spermatogonial stem cell marker PLZF (ZBTB16 – Mouse Genome Informatics) (Buaas et al., 2004; Costoya et al., 2004) (inset, Fig. 1B). BRG1 expression remained at 12 dpp as spermatocytes proceeded with meiosis (Fig. 1C). However, in adult testes, where all stages of spermatogenesis are present, BRG1 was detected predominantly in SYCP3-expressing meiocytes (Fig. 1D). BRG1 levels increased from zygonema to pachynema (Fig. 1E), during which DNA repair and recombination take place. We further analyzed the expression of the BRM ATPase subunit expression during spermatogenesis. In contrast to BRG1, it is expressed in somatic cells and differentiating spermatids, but not in wild-type spermatocytes (supplementary material Fig. S1). Thus, BRG1 and BRM may have complimentary, non-redundant roles during male meiosis. Together, these observations demonstrate that BRG1 is dynamically regulated during spermatogenesis, and its increased levels in spermatocytes suggest a role for BRG1 in the progression of meiosis.

Brg1 deficiency results in meiotic arrest

To determine whether BRG1 is required for spermatogenesis, we used a germ-cell-specific Cre recombinase to delete a *Brg1* floxed allele (Sumi-Ichinose et al., 1997) during embryonic germ cell

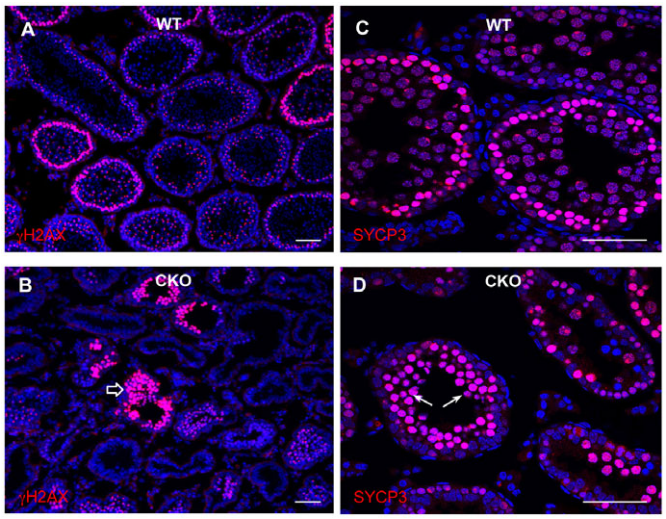

Fig. 3. *Brg1* mutant spermatocytes arrest at prophase of meiosis I. (**A-D**) Analysis of meiotic markers, γH2AX or SYCP3, in wild-type (A,C) and *Brg1*^{CKO} seminiferous tubules (B,D) of 2-week-old testes. Abnormal accumulation of γH2AX- and SYCP3-positive spermatocytes is indicated with block arrow and arrows, respectively (B,D).

development. *Mhv-Cre* (Gallardo et al., 2007) is expressed in primordial germ cells beginning at embryonic day 15.5. We confirmed the timing and specificity of *Mvh-Cre* using the R26R reporter gene (Soriano, 1997) (supplementary material Fig. S2). Morphological analysis of adult *Mvh-Cre/+; Brg1*$^{fl/\Delta}$ (referred to as *Brg1*^{CKO}) testes demonstrated a dramatic decrease in size relative to wild-type testes (Fig. 2A). Mutant seminiferous tubules contained spermatogonial cells and spermatocytes, but lacked fully differentiated cells such as round and elongated spermatids (Fig. 2B-E). In contrast to the robust BRG1 immunostaining in the testes of wild-type (*Brg1*$^{fl/\Delta}$) males lacking the Cre recombinase, testes of *Brg1*^{CKO} males showed BRG1 expression excluded from germ cells identified by expression of TRA98 – a pan-germ cell marker (Tanaka et al., 1997) (Fig. 2F,G). BRG1 was detected in somatic, TRA98-negative Sertoli cells (arrows in Fig. 2G), which do not express Cre, further demonstrating the specificity of *Mvh-Cre* directed excision. These results demonstrate that germ cells depleted for BRG1 are unable to complete spermatogenesis, and suggest that BRG1 is required for progression through meiosis.

To determine the cause of the arrest, we characterized spermatogenesis in *Brg1*^{CKO} mice at 7 dpp when testes are populated only by spermatogonia. Compared with littermate controls, mutant testes appeared to contain normal numbers of germ cells, as marked by TRA98 (supplementary material Fig. S3A,B). Moreover, the frequency of proliferating cells, marked by phospho-histone H3 (phosphorylated serine 10, histone H3), was also comparable (supplementary material Fig. S3C,D). Thus, *Brg1* appears dispensable for viability and proliferation of spermatogonia. We asked next whether differentiation of spermatogonia is affected in mutant testes. We observed comparable expression of the spermatocyte marker MVH (DDX4 – Mouse Genome Informatics) (Tanaka et al., 2000) (Fig. 2H,I) in 1-month-old testes from *Brg1*^{CKO} and control testes, indicating that mutant spermatocytes can initiate differentiation.

As mutant tubules lacked germ cells beyond the spermatocyte stage, we determined whether mutant spermatocytes were undergoing apoptosis. Using a TUNEL assay, we detected increased cell death in mutant testes compared with wild-type littermates (Fig. 2J,K). Some of the TUNEL-positive cells also stained positively for the spermatocyte marker SYCP3 (Fig. 2L). Therefore, deletion of *Brg1* impedes progression of spermatogenesis during meiotic stages, resulting in increased apoptosis.

Synapsis is impaired in *Brg1*^{CKO} spermatocytes

To determine whether mutant spermatocytes progress properly through prophase I, we analyzed the expression and localization patterns of meiotic markers. γH2AX levels are known to increase during leptonema, correlating with DSB formation, then diminish as breaks are repaired during zygonema, eventually becoming confined to the XY bivalent by the pachytene stage (Mahadevaiah et al., 2001; Celeste et al., 2002; Fernandez-Capetillo et al., 2003). We observed a pattern of γH2AX staining in *Brg1*^{CKO} tubules consistent with the leptotene stage of the first meiotic prophase. However, in contrast to wild-type tubules, where the normal pattern of the diffusely staining γH2AX in leptotene or zygotene spermatocytes is a single layer, we observed these cells accumulating in multiple layers in *Brg1*^{CKO} testes (Fig. 3A,B). We next assayed SYCP3, which is highly expressed in zygotene spermatocytes, becoming confined to the axes of paired chromosomes during pachynema. Similar to γH2AX staining, intensely staining SYCP3 spermatocytes accumulated abnormally in *Brg1*^{CKO} tubules (Fig. 3C,D).

To examine the defect more closely, we monitored meiotic progression by using spermatocyte spreads immunostained with markers for axial and transverse elements of the synaptonemal complex, SYCP3 and SYCP1, respectively. In wild-type spermatocytes, SYCP3 localization to chromosomal axes begins in the leptotene stage, continues along the aligning axes in the zygotene stage, and forms a condensed synaptonemal complex by the pachytene stage (Fig. 4A). Although SYCP3 patterns reflecting zygonema and pachynema could be detected in *Brg1*^{CKO} spermatocytes, localization of SYCP3 to the synaptonemal complex was abnormal (arrows in Fig. 4B). A significant increase in pachytene nuclei displaying asynapsis (70/80 nuclei) was observed in mutants compared with wild type (29/127 nuclei) (P<0.001, two-sided Fisher's exact test). Examination of SYCP1 localization, which becomes enriched at the transverse element bridging the two homologs together, confirmed that *Brg1*^{CKO} pachytene spermatocytes fail to produce a complete synaptonemal complex (compare Fig. 4C, wild type, with 4D, mutant, incomplete synaptonemal complex highlighted with arrows). Furthermore, after quantifying the stages of meiosis I from nuclear spreads, we did not observe any diplotene stage spermatocytes at 20 dpp in *Brg1*^{CKO} tubules (supplementary material Fig. S4). Together these observations demonstrate that synapsis is impaired in the absence of BRG1.

DNA repair is compromised in *Brg1*^{CKO} spermatocytes

A defect in processing of DSBs is often associated with abnormal synapsis (Baker et al., 1995; Burgoyne et al., 2009). BRG1-depleted zygotene spermatocytes consistently displayed prolonged γH2AX expression (Fig. 4B,D), implying that unrepaired DSBs are persistent and that deficiency in DNA repair might be linked to incomplete synapsis. Therefore, we used immunofluorescence to analyze levels and distribution of RAD51 (Shinohara et al., 1993) and replication protein A (RPA) (Plug et al., 1997), both of which are critical components of the DNA repair complex. RPA binds single-stranded DNA, and it is replaced by RAD51, which

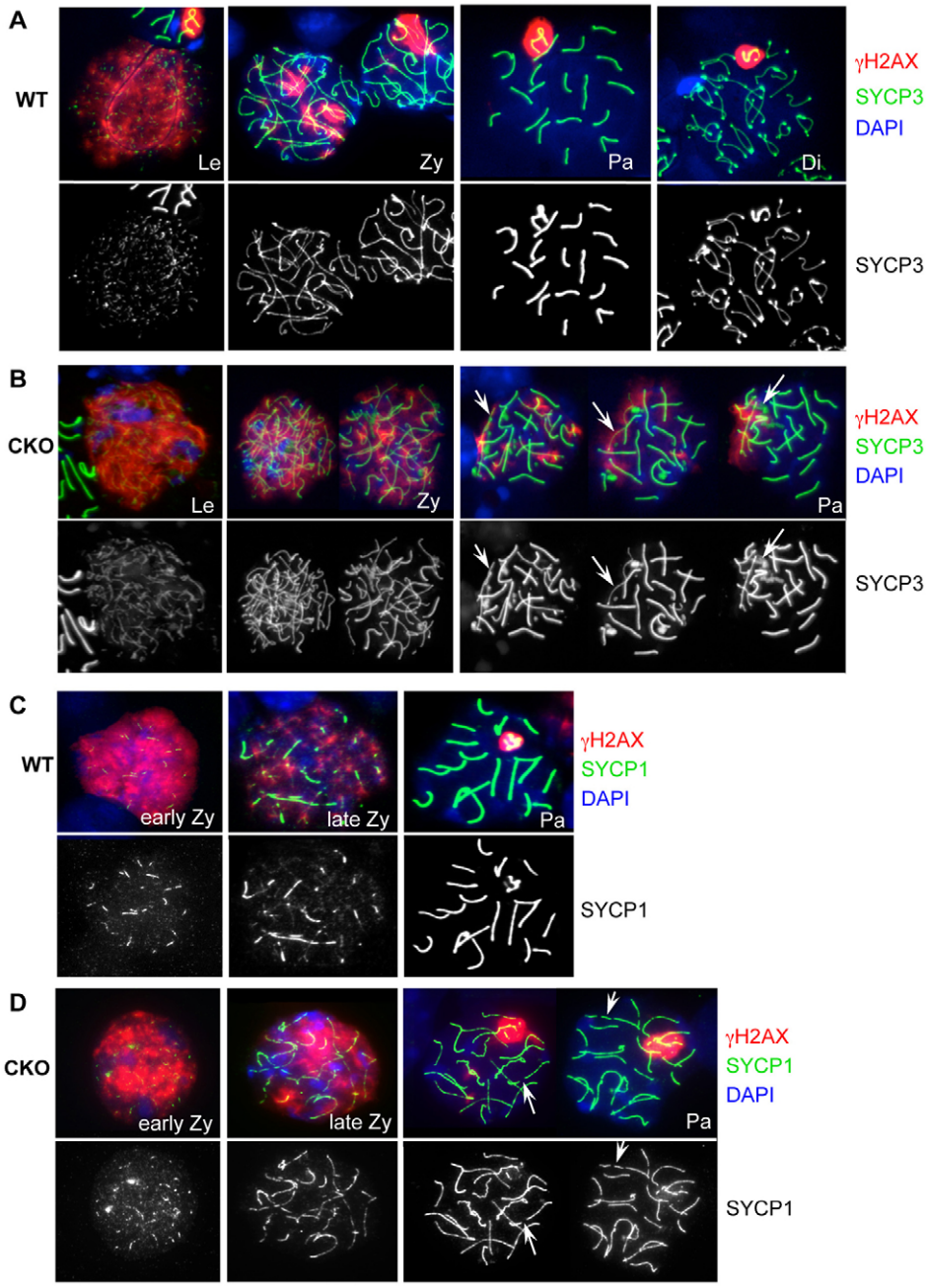

Fig. 4. *Brg1*^{CKO} spermatocytes fail to complete synapses. Distribution of the synaptonemal complex component, SYCP3 (green), and DSB marker, γH2AX (red), in nuclear spreads of 21 dpp wild-type (**A**) and *Brg1*^{CKO} (**B**) spermatocytes. Diplotene spermatocytes were not observed in *Brg1*^{CKO} testes. Localization of the transverse element of the synaptonemal complex SYCP1 (green), in preparations of 15 dpp wild-type (**C**) and *Brg1*^{CKO} (**D**) spermatocytes. Arrows in B and D indicate incomplete synapsis.

facilitates DNA strand exchange. Both factors showed irregular distribution and kinetics in mutant spermatocytes (Fig. 5A-D). Each formed enlarged and persistent foci between zygonema and pachynema, suggesting abnormal repair of DSBs (Petrini and Stracker, 2003). Notably, the exacerbated foci were associated with increasing synaptic defects (arrows in Fig. 5B,D). The majority of pachytene spermatocytes (58/79, 73%) contained multiple, enlarged RPA-foci accumulating to locally asynaptic axes. These patterns were never observed in wild-type spermatocytes.

In mouse, ~300 DSBs per leptotene nucleus are generated by SPO11 (Keeney, 2001). DNA repair generates two alternative recombination products, crossover (CO, <10% of all the DSBs) or non-crossover (NCO) (Moens et al., 2002). To compare wild-type and *Brg1*^{CKO} recombination patterns, distribution of the recombination protein MLH1 was examined. MLH1 specifically marks CO-designated sites in mid to late pachytene spermatocytes (Moens et al., 2007). Although CO formation in *Brg1*^{CKO} spermatocytes was readily observed, the average number of MLH1 foci in each nucleus was significantly reduced in mutant pachytene spermatocytes compared with controls (Fig. 5E-G, 17.3 versus 21.1 MLH1 foci/spermatocyte, $P=2.3\times10^{-6}$). Mutant nuclei with fewer than 20 MLH1 foci displayed extensive asynapsis, suggesting that the decrease in MLH1 foci among mutant spermatocytes is likely to be a consequence of delayed synaptic progression, possibly linked to deficiency in DNA repair.

Brg1^{CKO} spermatocytes show abnormal chromatin modifications

SWI/SNF chromatin remodelers such as BRG1 are thought to produce a more open chromatin structure (Bultman et al., 2006). To determine whether the failure in meiotic progression correlated with changes in chromatin structure in the absence of BRG1, we

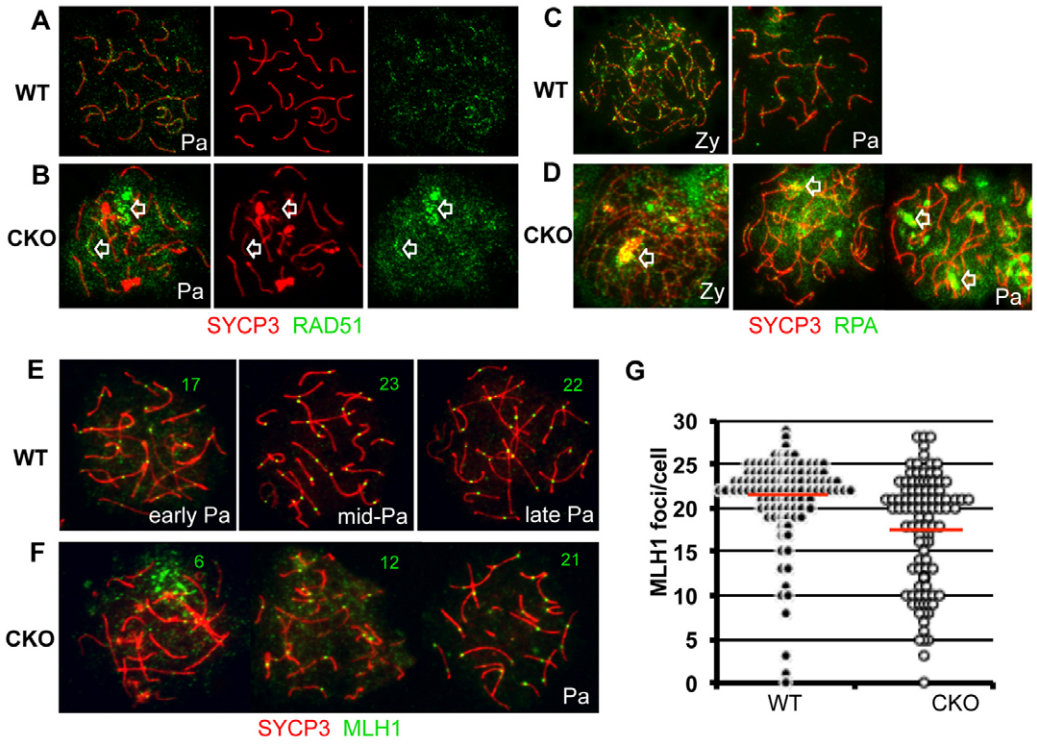

Fig. 5. Ectopic accumulation of DNA repair factors in *Brg1*^{CKO} spermatocytes. (**A-D**) Distribution of repair proteins RAD51 (green; A,B) and RPA (green; C,D) in wild-type (A,C) and *Brg1*^{CKO} (B,D) spermatocytes. SYCP3 (red) was used in nuclear spreads to identify spermatocytes in the zygotene or pachytene stages. Arrowheads in B and D depict abnormal repair foci of *Brg1*^{CKO}. (**E**,**F**) Crossover formation in pachytene spermatocytes. MLH1-containing recombination nodules (green) on the synaptic axes (red) in wild-type (E) and mutant spermatocytes (F) are shown in nuclei spreads prepared from 15 dpp testis. Numbers in representative images (E,F) indicate the number of MLH1 foci per nucleus. (**G**) Beeswarm plot of MLH1 foci in each control (black circle, n=110) and *Brg1*^{CKO} (open circle, n=108) spermatocyte. The red line is the average number of MLH1 foci in each genotype (21.1 in wild type versus 17.3 in *Brg1*^{CKO}; P=2.3x10^{-6}); statistical significance was determined by t-test. Pa, pachynema; Zy, zygonema.

examined global patterns of histone modifications and chromatin-binding proteins. We first investigated acetylation of lysine 14 of histone H3 (H3K14Ac), a modification thought to facilitate the recruitment of DNA damage response proteins (Lee et al., 2010; Buard et al., 2009). We found that, although H3K14Ac was induced in mutant spermatocytes, it persisted abnormally into the pachytene stage (Fig. 6A,B). Similarly, dimethylation at histone H3K9 (H3K9me2), a heterochromatin-associated modification, was also abnormally increased in mutant tubules (Fig. 6C,D). Staging nuclear spreads with SYCP3 revealed that this upregulation occurred during the zygotene stage, preceding the period of ectopically increased H3K14Ac (Fig. 6E,F).

Heterochromatin protein 1 (HP1; CBX5 – Mouse Genome Informatics) is a non-histone protein that regulates the assembly of heterochromatin (Zhao et al., 2000). We examined expression of all three members of mammalian HP1 proteins: HP1α, HP1β and HP1γ. HP1α expression was negligible in both wild-type and mutant spermatocytes (data not shown). In wild-type tubules, HP1β and HP1γ strongly stained cells at the base of the lamina with levels decreasing as cells entered meiosis and moved towards the lumen. Only HP1β was reactivated in pachytene spermatocytes (Fig. 6G). In *Brg1*^{CKO} tubules, broad staining of both HP1β and HP1γ persisted into spermatocytes (arrows in Fig. 6H), which contained abnormally high levels of γH2AX (Fig. 6J). Taken together, these results show differences in the patterns of histone modifications in the absence of BRG1 during meiosis and suggest a more closed, heterochromatic state.

DISCUSSION

Chromatin-remodeling proteins have significant roles in facilitating DSB repair and maintaining genome stability (Downs et al., 2007). Here, we demonstrate an essential role for a catalytic subunit of the mammalian SWI/SNF complex, BRG1, during the programmed DNA damage events of meiosis in the male germline. Although DSB repair appears to begin normally in *Brg1*^{CKO} spermatocytes, DNA damage persists into later stages of prophase I, as indicated by persistent γH2AX, unresolved repair foci and damage-associated H3K14Ac, suggesting that DSB repair is unable to proceed to completion. Subsequently, progression through the first meiotic prophase of *Brg1*^{CKO} spermatocytes is blocked, resulting in the elimination of the spermatocytes presumably by meiotic checkpoint-triggered cell death. Recombination and synapsis are mutually interdependent, such that the resolution of recombination intermediates requires assembly of intact synaptonemal complexes (Plug et al., 1998). Unrepaired DSBs in the *Brg1*^{CKO} mutants might result from incomplete synapsis, deficiency in DNA repair, or some defect upstream of synapsis/repair. Intriguingly, we observed the presence of crossover sites, as measured by MLH1 foci, in *Brg1*^{CKO} mutant spermatocytes despite measurable asynapsis. It is possible, therefore, that BRG1 is specifically required for synapsis in condensed, heterochromatic domains.

Previously, Park *et al* demonstrated that upon induction of DSBs by ionizing radiation, BRG1 is required to promote high levels of γH2AX for efficient repair (Park et al., 2006). In contrast, we observe that γH2AX appears normally in *Brg1*^{CKO} spermatocytes during the

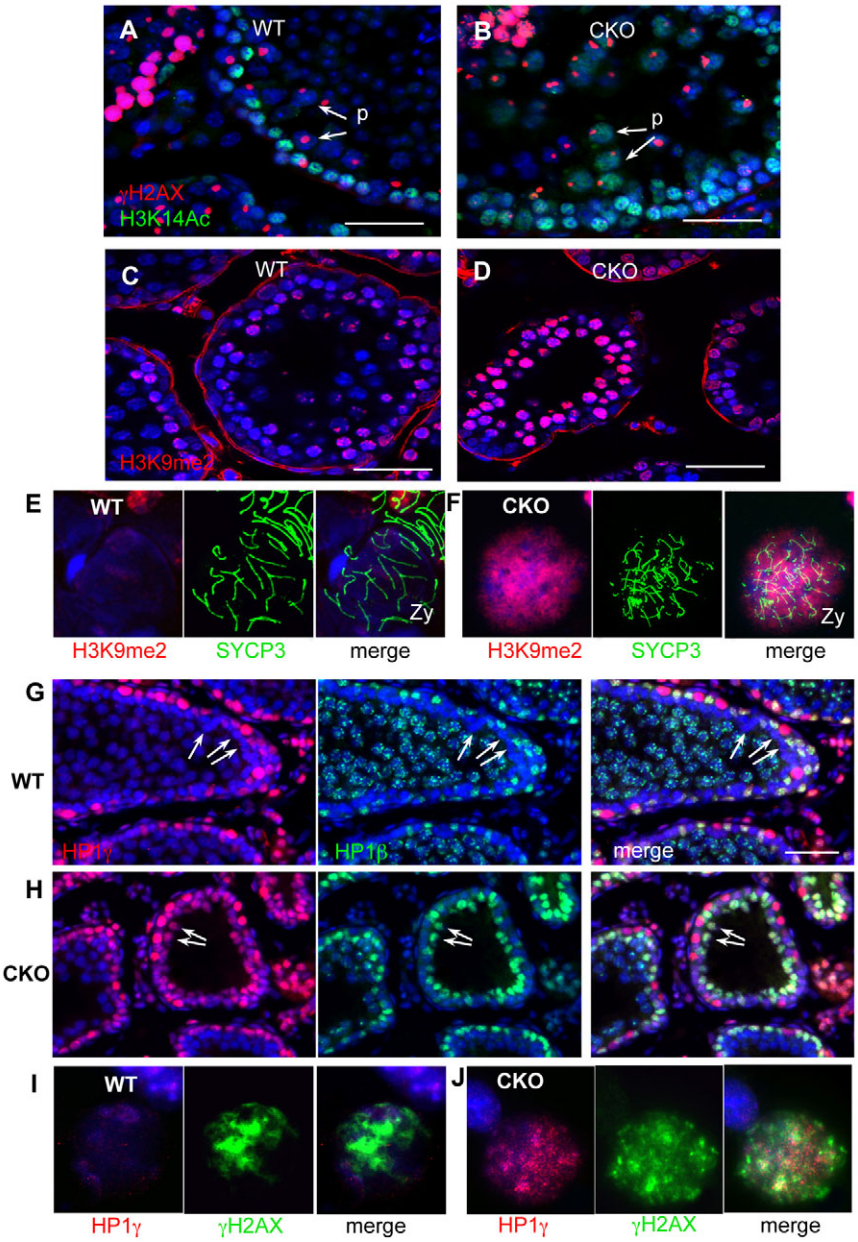

Fig. 6. Increased distribution of heterochromatic histone modifications and HP1 proteins in *Brg1*^{CKO} spermatocytes. H4K14Ac (green), a mark associated with DNA repair, in wild-type (**A**) and *Brg1*^{CKO} (**B**) adult testes. Spermatocytes are identified by γH2AX staining (red). Arrows show pachytene spermatocytes. H3K9me2 (red) in wild-type (**C**) and mutant (**D**) testes at 14 dpp. H3K9me2 distribution in wild-type (**E**) and *Brg1*^{CKO} (**F**) zygotene spermatocytes. Expression of HP1γ (red) and HP1β (green) in 14 dpp wild-type (**G**) and *Brg1*^{CKO} (**H**) tubules. Broad staining persisted in mutant spermatocysts (G,H, arrows). Distribution of HP1γ (red) in wild-type (**I**) and mutant (**J**) zygonema spermatocytes.

leptotene stage of meiosis. However, γH2AX distribution was abnormal. Instead of being normally displaced from autosomes and confined to the XY body, γH2AX remained broadly dispersed in mutant zygotene spermatocytes and into the pachytene stage. Therefore, during meiosis, BRG1 appears to function downstream of γH2AX accumulation. This discrepancy may reflect mechanistic differences in DNA repair that occur in response to stress and those that occur during meiosis (Andersen and Sekelsky, 2010). The timing of BRG1 requirement during meiotic DSB repair is reminiscent of that observed in yeast. In this organism, the SWI/SNF remodeling complex appears to be involved later in the DSB repair process, perhaps during or after the invasion of single-stranded DNA to donor DNA (Chai et al., 2005).

We have previously observed differences in the histone modifications of BRG1-depleted embryos (Bultman et al., 2006). Here, we show that *Brg1*^{CKO} spermatocytes undergo changes in heterochromatin-associated histone modification patterns. These observations suggest a more condensed chromatin state relative to wild-type spermatocytes. Heterochromatic regions require SWI/SNF complexes to complete recombination in yeast (Sinha et al., 2009). Thus, the defect in DNA repair coupled with the increased heterochromatic nature of *Brg1*^{CKO} spermatocytes suggest that mammalian SWI/SNF complexes perhaps facilitate DSB repair and recombination in more condensed genomic contexts. Together, our results suggest an essential role for the BRG1 ATPase in mammalian male meiosis.

Acknowledgements
We thank the members of the Magnuson Lab for critical reading of the manuscript; Joshua Starmer for statistical analysis; Dale A. Ramsden (UNC) for anti-Rad51 antibody; Dr D. H. Castrillon (UT Southwestern for the *Mhv-Cre* line, provided by Dr Blanche Capel, Duke University); and Dr Pierre Chambon (Strasbourg) for *Brg1*^{flox} mice.

Funding
This work was supported by a National Institutes of Health grant [HD036655 to T.M.] and a National Research Service Award (NRSA) Fellowship [HD0052413 to A.M.F.] Deposited in PMC for release after 12 months.

Competing interests statement
The authors declare no competing financial interests.

Supplementary material
Supplementary material available online at
http://dev.biologists.org/lookup/suppl/doi:10.1242/dev.073478/-/DC1

References

Andersen, S. L. and Sekelsky, J. (2010). Meiotic versus mitotic recombination: two different routes for double-strand break repair: the different functions of meiotic versus mitotic DSB repair are reflected in different pathway usage and different outcomes. *BioEssays* **32**, 1058-1066.
Baker, S. M., Bronner, C. E., Zhang, L., Plug, A. W., Robatzek, M., Warren, G., Elliott, E. A., Yu, J., Ashley, T., Arnheim, N. et al. (1995). Male mice defective in the DNA mismatch repair gene PMS2 exhibit abnormal chromosome synapsis in meiosis. *Cell* **82**, 309-319.
Bao, Y. and Shen, X. (2007). Chromatin remodeling in DNA double-strand break repair. *Curr. Opin. Genet. Dev.* **17**, 126-131.
Buaas, F. W., Kirsh, A. L., Sharma, M., McLean, D. J., Morris, J. L., Griswold, M. D., de Rooij, D. G. and Braun, R. E. (2004). Plzf is required in adult male germ cells for stem cell self-renewal. *Nat. Genet.* **36**, 647-652.
Buard, J., Barthes, P., Grey, C. and de Massy, B. (2009). Distinct histone modifications define initiation and repair of meiotic recombination in the mouse. *EMBO J.* **28**, 2616-2624.
Bultman, S. J., Gebuhr, T. C., Pan, H., Svoboda, P., Schultz, R. M. and Magnuson, T. (2006). Maternal BRG1 regulates zygotic genome activation in the mouse. *Genes Dev.* **20**, 1744-1754.
Burgoyne, P. S., Mahadevaiah, S. K. and Turner, J. M. (2009). The consequences of asynapsis for mammalian meiosis. *Nat. Rev. Genet.* **10**, 207-216.
Celeste, A., Petersen, S., Romanienko, P. J., Fernandez-Capetillo, O., Chen, H. T., Sedelnikova, O. A., Reina-San-Martin, B., Coppola, V., Meffre, E., Difilippantonio, M. J. et al. (2002). Genomic instability in mice lacking histone H2AX. *Science* **296**, 922-927.
Chai, B., Huang, J., Cairns, B. R. and Laurent, B. C. (2005). Distinct roles for the RSC and Swi/Snf ATP-dependent chromatin remodelers in DNA double-strand break repair. *Genes Dev.* **19**, 1656-1661.
Clapier, C. R. and Cairns, B. R. (2009). The biology of chromatin remodeling complexes. *Annu. Rev. Biochem.* **78**, 273-304.
Costoya, J. A., Hobbs, R. M., Barna, M., Cattoretti, G., Manova, K., Sukhwani, M., Orwig, K. E., Wolgemuth, D. J. and Pandolfi, P. P. (2004). Essential role of Plzf in maintenance of spermatogonial stem cells. *Nat. Genet.* **36**, 653-659.
Downs, J. A., Nussenzweig, M. C. and Nussenzweig, A. (2007). Chromatin dynamics and the preservation of genetic information. *Nature* **447**, 951-958.
Fernandez-Capetillo, O., Mahadevaiah, S. K., Celeste, A., Romanienko, P. J., Camerini-Otero, R. D., Bonner, W. M., Manova, K., Burgoyne, P. and Nussenzweig, A. (2003). H2AX is required for chromatin remodeling and inactivation of sex chromosomes in male mouse meiosis. *Dev. Cell* **4**, 497-508.
Gallardo, T., Shirley, L., John, G. B. and Castrillon, D. H. (2007). Generation of a germ cell-specific mouse transgenic Cre line, Vasa-Cre. *Genesis* **45**, 413-417.
Keeney, S. (2001). Mechanism and control of meiotic recombination initiation. *Curr. Top. Dev. Biol.* **52**, 1-53.
Kim, Y., Bingham, N., Sekido, R., Parker, K. L., Lovell-Badge, R. and Capel, B. (2007). Fibroblast growth factor receptor 2 regulates proliferation and Sertoli differentiation during male sex determination. *Proc. Natl. Acad. Sci. USA* **104**, 16558-16563.
Kota, S. K. and Feil, R. (2010). Epigenetic transitions in germ cell development and meiosis. *Dev. Cell* **19**, 675-686.
Lee, H. S., Park, J. H., Kim, S. J., Kwon, S. J. and Kwon, J. (2010). A cooperative activation loop among SWI/SNF, gamma-H2AX and H3 acetylation for DNA double-strand break repair. *EMBO J.* **29**, 1434-1445.
Mahadevaiah, S. K., Turner, J. M., Baudat, F., Rogakou, E. P., de Boer, P., Blanco-Rodriguez, J., Jasin, M., Keeney, S., Bonner, W. M. and Burgoyne, P. S. (2001). Recombinational DNA double-strand breaks in mice precede synapsis. *Nat. Genet.* **27**, 271-276.
Moens, P. B., Kolas, N. K., Tarsounas, M., Marcon, E., Cohen, P. E. and Spyropoulos, B. (2002). The time course and chromosomal localization of recombination-related proteins at meiosis in the mouse are compatible with models that can resolve the early DNA-DNA interactions without reciprocal recombination. *J. Cell Sci.* **115**, 1611-1622.
Moens, P. B., Marcon, E., Shore, J. S., Kochakpour, N. and Spyropoulos, B. (2007). Initiation and resolution of interhomolog connections: crossover and non-crossover sites along mouse synaptonemal complexes. *J. Cell Sci.* **120**, 1017-1027.
Park, J. H., Park, E. J., Lee, H. S., Kim, S. J., Hur, S. K., Imbalzano, A. N. and Kwon, J. (2006). Mammalian SWI/SNF complexes facilitate DNA double-strand break repair by promoting gamma-H2AX induction. *EMBO J.* **25**, 3986-3997.
Peters, A. H., Plug, A. W., van Vugt, M. J. and de Boer, P. (1997). A drying-down technique for the spreading of mammalian meiocytes from the male and female germline. *Chromosome Res.* **5**, 66-68.
Petrini, J. H. and Stracker, T. H. (2003). The cellular response to DNA double-strand breaks: defining the sensors and mediators. *Trends Cell Biol.* **13**, 458-462.
Plug, A. W., Peters, A. H., Xu, Y., Keegan, K. S., Hoekstra, M. F., Baltimore, D., de Boer, P. and Ashley, T. (1997). ATM and RPA in meiotic chromosome synapsis and recombination. *Nat. Genet.* **17**, 457-461.
Plug, A. W., Peters, A. H., Keegan, K. S., Hoekstra, M. F., de Boer, P. and Ashley, T. (1998). Changes in protein composition of meiotic nodules during mammalian meiosis. *J. Cell Sci.* **111**, 413-423.
Sasaki, H. and Matsui, Y. (2008). Epigenetic events in mammalian germ-cell development: reprogramming and beyond. *Nat. Rev. Genet.* **9**, 129-140.
Shinohara, A., Ogawa, H., Matsuda, Y., Ushio, N., Ikeo, K. and Ogawa, T. (1993). Cloning of human, mouse and fission yeast recombination genes homologous to RAD51 and recA. *Nat. Genet.* **4**, 239-243.
Sinha, M., Watanabe, S., Johnson, A., Moazed, D. and Peterson, C. L. (2009). Recombinational repair within heterochromatin requires ATP-dependent chromatin remodeling. *Cell* **138**, 1109-1021.
Soriano, P. (1997). The PDGF alpha receptor is required for neural crest cell development and for normal patterning of the somites. *Development* **124**, 2691-2700.
Sumi-Ichinose, C., Ichinose, H., Metzger, D. and Chambon, P. (1997). SNF2beta-BRG1 is essential for the viability of F9 murine embryonal carcinoma cells. *Mol. Cell. Biol.* **17**, 5976-5986.
Tanaka, H., Pereira, L. A., Nozaki, M., Tsuchida, J., Sawada, K., Mori, H. and Nishimune, Y. (1997). A germ cell-specific nuclear antigen recognized by a monoclonal antibody raised against mouse testicular germ cells. *Int. J. Androl.* **20**, 361-366.
Tanaka, S. S., Toyooka, Y., Akasu, R., Katoh-Fukui, Y., Nakahara, Y., Suzuki, R., Yokoyama, M. and Noce, T. (2000). The mouse homolog of Drosophila Vasa is required for the development of male germ cells. *Genes Dev.* **14**, 841-853.
Zhao, Q., Wang, Q. E., Ray, A., Wani, G., Han, C., Milum, K. and Wani, A. A. (2009). Modulation of nucleotide excision repair by mammalian SWI/SNF chromatin-remodeling complex. *J. Biol. Chem.* **284**, 30424-30432.
Zhao, T., Heyduk, T., Allis, C. D. and Eissenberg, J. C. (2000). Heterochromatin protein 1 binds to nucleosomes and DNA in vitro. *J. Biol. Chem.* **275**, 28332-28338.